Phosphorus and silicon-bridged stilbenes: synthesis and optoelectronic properties

Yang Zhou[a], Shuai Yang[b] Jun Li[a], Gufeng He[b], Zheng Duan*[a], Francois Mathey*[a,c]*

a) College of Chemistry and Molecular Engineering, International Phosphorus Laboratory, International Joint Research Laboratory for Functional Organophosphorus Materials of Henan Province, Zhengzhou University, Zhengzhou 450001, P. R. China;

b) National Engineering Lab for TFT-LCD Materials and Technologies, Department of Electronic Engineering, Shanghai Jiao Tong University, Shanghai 200240, P. R. China;

c) Division of Chemistry & Biological Chemistry, Nanyang Technological University, 21 Nanyang Link, Singapore 637371

gufenghe@sjtu.edu.cn ; duanzheng@zzu.edu.cn; fmathey@ntu.edu.sg

Table of Contents Page **Page**

TGA and DSC

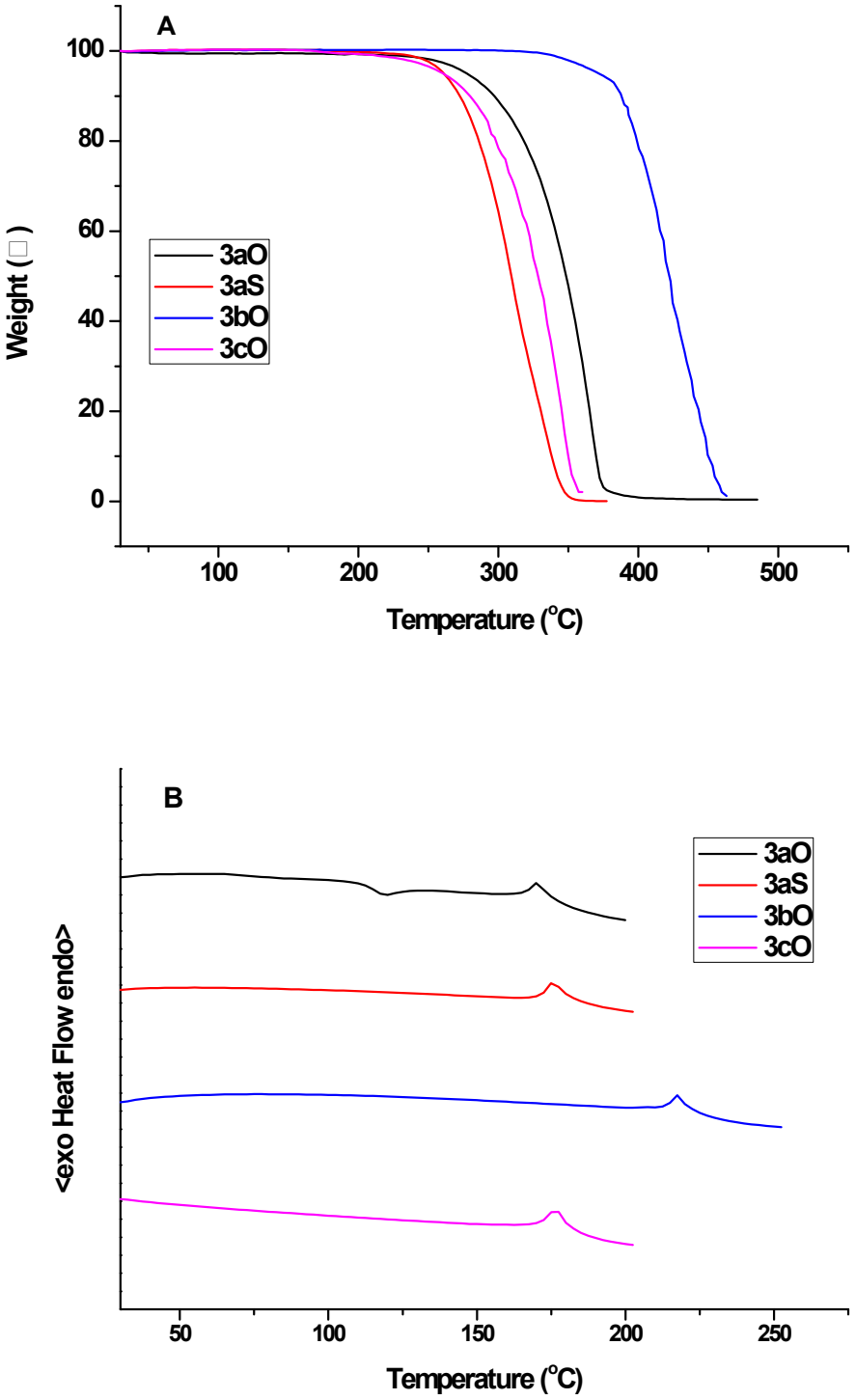

Figure S1. TGA (**A**) and DSC (**B**) of **3aO**, **3aS**, **3bO**, **3cO** under dry nitrogen at a Heating rate of 10 °C/min.

Table S1. Melting point and decomposition temperature of **3aO**, **3aS**, **3bO**, **3cO**.

Comp.	T^{a}_{m}[°C]	T^{b}_{m}[°C]	T^{c}_{d}[°C]
3aO	170	172	277
3aS	175	179	260
3bO	217	214	372
3cO	176	178	260

[a]Melting point were performed by DSC. [b]Melting point were obtained on an X-4 micro-melting point apparatus.

[c]Decomposition temperature were defined as 5% of weigh loss under argon, 10 °C/min.

Electrochemical properties

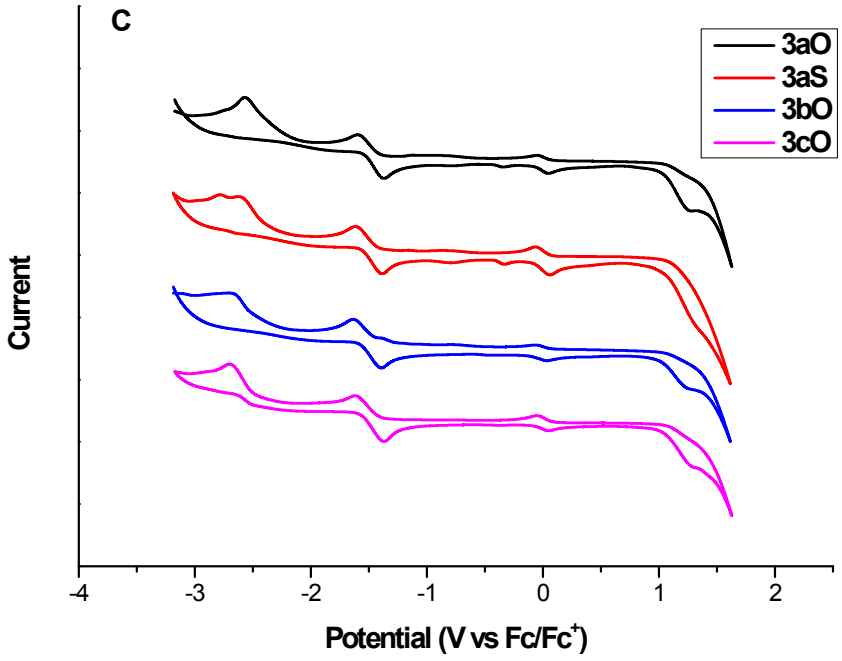

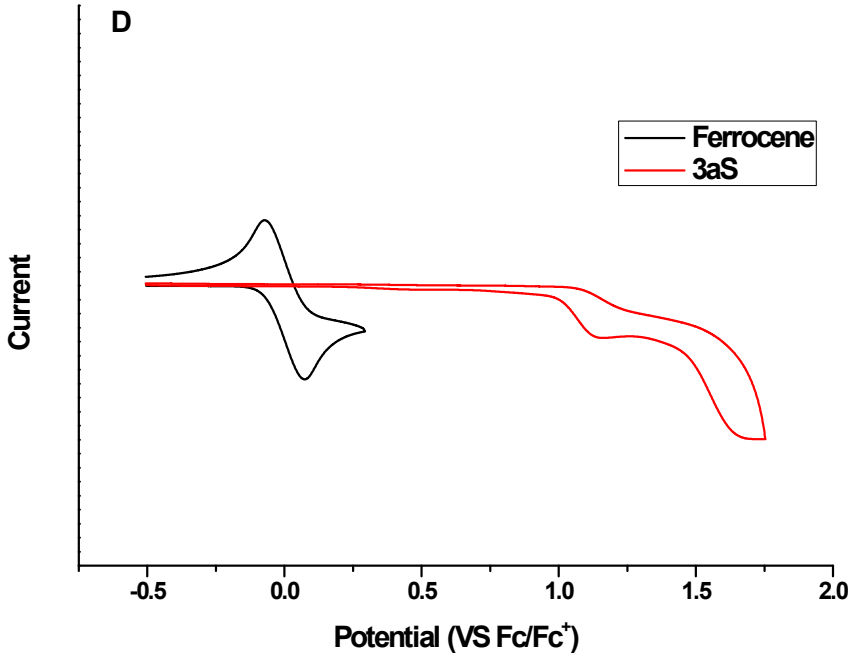

Figure S2. Cyclic voltammograms (**C**) of **3aO**, **3aS**, **3bO**, **3cO** (vs Fc/Fc^+, Solvent: THF, Scan rate: 50 mV/s); Oxidation Potential (**D**) of **3aS** (vs Fc/Fc^+, Solvent: CH_2Cl_2, San rate: 50 Mv/s).

X-ray Crystallographic Studies of Compound 1:

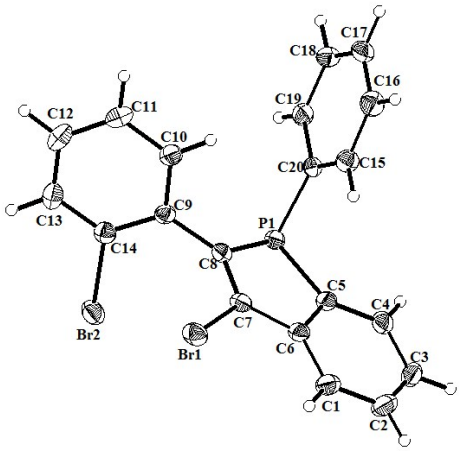

Figure S3. X-ray Crystal structure of **1.** The level set for thermal ellipsoids of all atoms is 30%.

Table S2. Crystal data and structure refinement for **1**.

Identification code	1
Chemical formula	$C_{20}H_{13}Br_2P$
Formula weight	444.09 g/mol
Temperature	170(2) K
Wavelength	1.54178 Å
Crystal system	triclinic

Space group	P -1
a	9.4809(3) Å
b	10.1007(3) Å
c	10.6941(3) Å
α	100.8620(10)°
β	108.6480(10)°
γ	110.1290(10)°
Volume	858.26(4) $Å^3$
Z	2
Density (calculated)	1.718 g/cm^3
Absorption coefficient	6.825 mm^{-1}
F(000)	436
Theta range for data collection	4.63 to 68.33°
Index ranges	-11<=h<=10, -12<=k<=12, -12<=l<=12
Reflections collected	9719
Independent reflections	3130 [R(int) = 0.0236]
Coverage of independent reflections	99.50%
Absorption correction	Multi-Scan
Refinement method	Full-matrix least-squares on F^2
Refinement program	SHELXL-2014/7 (Sheldrick, 2014)
Function minimized	$\Sigma w(F_o^2 - F_c^2)^2$
Data / restraints / parameters	3130 / 0 / 208
Goodness-of-fit on F^2	1.1
Δ/σ_{max}	0.001
Final R indices[I>2σ(I)]	R1 = 0.0211, wR2 = 0.0542
Final R indices[all data]	R1 = 0.0226, wR2 = 0.0550
Largest diff. peak and hole	0.285 and -0.556 $eÅ^{-3}$

Table S3. Bond Lengths for **1**.

Br1-C20	1.903(2)	Br2-C18	1.9061(19)
P1-C12	1.8212(19)	P1-C5	1.833(2)
P1-C4	1.8375(19)	C1-C11	1.381(3)
C1-C2	1.384(3)	C1-H1	0.95
C2-C3	1.387(3)	C2-H13	0.95
C3-C4	1.392(3)	C3-H12	0.95
C4-C10	1.393(3)	C5-C18	1.340(3)

C5-C6	1.482(3)	C6-C20	1.392(3)
C6-C7	1.402(3)	C7-C8	1.383(3)
C7-H11	0.95	C8-C9	1.383(3)
C8-H10	0.95	C9-C19	1.387(3)
C9-H2	0.95	C10-C11	1.392(3)
C10-H4	0.95	C11-H3	0.95
C12-C17	1.388(3)	C12-C13	1.403(3)
C13-C14	1.393(3)	C13-C18	1.460(3)
C14-C15	1.386(3)	C14-H8	0.95
C15-C16	1.385(3)	C15-H7	0.95
C16-C17	1.394(3)	C16-H6	0.95
C17-H5	0.95	C19-C20	1.386(3)
C19-H9	0.95		

Table S4. Bond Angles for **1**.

C12-P1-C5	90.00(9)	C12-P1-C4	104.52(9)
C5-P1-C4	101.01(8)	C11-C1-C2	119.95(19)
C11-C1-H1	120	C2-C1-H1	120
C1-C2-C3	120.0(2)	C1-C2-H13	120
C3-C2-H13	120	C2-C3-C4	120.34(18)
C2-C3-H12	119.8	C4-C3-H12	119.8
C3-C4-C10	119.52(18)	C3-C4-P1	122.95(15)
C10-C4-P1	117.45(14)	C18-C5-C6	128.08(18)
C18-C5-P1	109.92(15)	C6-C5-P1	121.95(14)
C20-C6-C7	117.25(18)	C20-C6-C5	123.12(17)
C7-C6-C5	119.61(17)	C8-C7-C6	121.18(19)
C8-C7-H11	119.4	C6-C7-H11	119.4
C9-C8-C7	120.2(2)	C9-C8-H10	119.9
C7-C8-H10	119.9	C8-C9-C19	119.86(19)
C8-C9-H2	120.1	C19-C9-H2	120.1
C11-C10-C4	119.67(18)	C11-C10-H4	120.2
C4-C10-H4	120.2	C1-C11-C10	120.51(19)
C1-C11-H3	119.7	C10-C11-H3	119.7
C17-C12-C13	120.10(18)	C17-C12-P1	128.41(16)
C13-C12-P1	111.07(14)	C14-C13-C12	120.44(19)
C14-C13-C18	128.31(19)	C12-C13-C18	111.24(17)
C15-C14-C13	118.9(2)	C15-C14-H8	120.5

C13-C14-H8	120.5	C16-C15-C14	120.9(2)
C16-C15-H7	119.6	C14-C15-H7	119.6
C15-C16-C17	120.5(2)	C15-C16-H6	119.7
C17-C16-H6	119.7	C12-C17-C16	119.1(2)
C12-C17-H5	120.4	C16-C17-H5	120.4
C5-C18-C13	117.23(18)	C5-C18-Br2	122.91(15)
C13-C18-Br2	119.85(14)	C20-C19-C9	119.4(2)
C20-C19-H9	120.3	C9-C19-H9	120.3
C19-C20-C6	122.04(19)	C19-C20-Br1	117.96(16)
C6-C20-Br1	120.00(15)		

X-ray Crystallographic Studies of Compound 3aO:

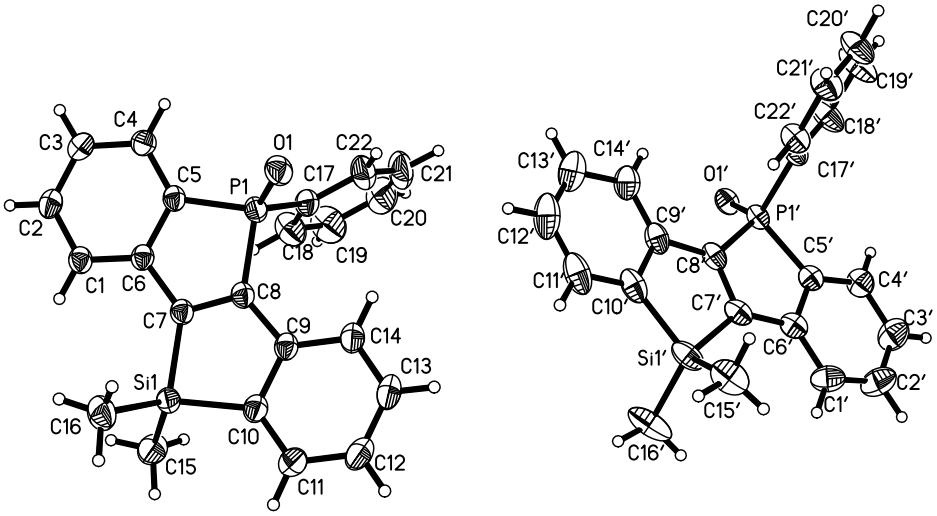

Figure S4. X-ray Crystal structure of **3aO.** The level set for thermal ellipsoids of all atoms is 30%.

Table S5. Crystal data and structure refinement for **3aO**.

dentification code	3aO
Empirical formula	$C_{22}H_{19}OPSi$
Formula weight	358.43
Temperature/K	291.15
Crystal system	triclinic
Space group	P-1
a/Å	10.2464(4)
b/Å	12.4270(6)
c/Å	17.6262(7)
α/°	84.434(3)
β/°	76.892(3)

γ/°	77.143(4)
Volume/Å^3	2128.52(15)
Z	4
ρ_{calc}g/cm^3	1.119
μ/mm^{-1}	1.718
F(000)	752
Crystal size/mm^3	0.22 × 0.2 × 0.17
Radiation	CuKα (λ = 1.54184)
2Θ range for data collection/°	7.3 to 134.14
Index ranges	-8 ≤ h ≤ 12, -14 ≤ k ≤ 14, -21 ≤ l ≤ 21
Reflections collected	15415
Independent reflections	7602 [R_{int} = 0.0225, R_{sigma} = 0.0311]
Data/restraints/parameters	7602/0/455
Goodness-of-fit on F^2	1.044
Final R indexes [I>=2σ (I)]	R_1 = 0.0414, wR_2 = 0.1161
Final R indexes [all data]	R_1 = 0.0498, wR_2 = 0.1231
Largest diff. peak/hole / e Å^{-3}	0.29/-0.23

Table S6. Bond Lengths for **3aO**.

Atom	Atom	Length/Å	Atom	Atom	Length/Å
P1	O1	1.4811(14)	P1'	O1'	1.4885(13)
P1	C5	1.8089(18)	P1'	C5'	1.809(2)
P1	C8	1.8059(19)	P1'	C8'	1.8110(18)
P1	C17	1.8141(19)	P1'	C17'	1.7972(18)
Si1	C7	1.8766(19)	Si1'	C7'	1.8834(19)
Si1	C10	1.8817(19)	Si1'	C10'	1.873(3)
Si1	C15	1.848(2)	Si1'	C15'	1.856(3)
Si1	C16	1.855(2)	Si1'	C16'	1.857(2)
C1	C2	1.398(3)	C1'	C2'	1.392(4)
C1	C6	1.385(2)	C1'	C6'	1.379(3)
C2	C3	1.375(3)	C2'	C3'	1.373(4)
C3	C4	1.397(3)	C3'	C4'	1.381(3)
C4	C5	1.376(3)	C4'	C5'	1.383(3)
C5	C6	1.403(3)	C5'	C6'	1.405(3)
C6	C7	1.483(2)	C6'	C7'	1.471(3)
C7	C8	1.353(3)	C7'	C8'	1.353(3)
C8	C9	1.473(3)	C8'	C9'	1.477(3)
C9	C10	1.408(3)	C9'	C10'	1.415(3)
C9	C14	1.394(3)	C9'	C14'	1.379(3)
C10	C11	1.385(3)	C10'	C11'	1.393(3)
C11	C12	1.391(3)	C11'	C12'	1.376(4)

C12	C13	1.373(3)	C12'	C13'	1.374(4)
C13	C14	1.388(3)	C13'	C14'	1.392(3)
C17	C18	1.381(3)	C17'	C18'	1.382(3)
C17	C22	1.374(3)	C17'	C22'	1.383(3)
C18	C19	1.382(3)	C18'	C19'	1.378(3)
C19	C20	1.372(4)	C19'	C20'	1.377(3)
C20	C21	1.350(4)	C20'	C21'	1.362(3)
C21	C22	1.409(4)	C21'	C22'	1.384(3)

Table S7. Bond Angles for **3aO**.

O1	P1	C5	118.28(8)	O1'	P1'	C5'	115.80(8)
O1	P1	C8	117.66(9)	O1'	P1'	C8'	117.77(8)
O1	P1	C17	113.35(10)	O1'	P1'	C17'	112.39(9)
C5	P1	C17	107.41(9)	C5'	P1'	C8'	91.68(9)
C8	P1	C5	91.57(8)	C17'	P1'	C5'	108.48(9)
C8	P1	C17	106.04(9)	C17'	P1'	C8'	108.76(8)
C7	Si1	C10	90.82(8)	C10'	Si1'	C7'	90.51(9)
C15	Si1	C7	116.01(10)	C15'	Si1'	C7'	113.23(11)
C15	Si1	C10	113.17(10)	C15'	Si1'	C10'	113.54(12)
C15	Si1	C16	111.36(12)	C15'	Si1'	C16'	111.87(13)
C16	Si1	C7	110.24(10)	C16'	Si1'	C7'	112.77(11)
C16	Si1	C10	113.84(11)	C16'	Si1'	C10'	113.35(15)
C6	C1	C2	118.72(18)	C6'	C1'	C2'	118.9(2)
C3	C2	C1	121.24(18)	C3'	C2'	C1'	121.2(2)
C2	C3	C4	120.30(18)	C2'	C3'	C4'	120.6(2)
C5	C4	C3	118.63(18)	C3'	C4'	C5'	118.6(2)
C4	C5	P1	128.93(15)	C4'	C5'	P1'	129.65(17)
C4	C5	C6	121.40(17)	C4'	C5'	C6'	121.1(2)
C6	C5	P1	109.63(13)	C6'	C5'	P1'	109.29(14)
C1	C6	C5	119.64(17)	C1'	C6'	C5'	119.6(2)
C1	C6	C7	127.00(17)	C1'	C6'	C7'	126.8(2)
C5	C6	C7	113.33(15)	C5'	C6'	C7'	113.65(18)
C6	C7	Si1	136.97(13)	C6'	C7'	Si1'	136.49(16)
C8	C7	Si1	108.46(14)	C8'	C7'	Si1'	108.95(15)
C8	C7	C6	114.05(16)	C8'	C7'	C6'	114.54(17)
C7	C8	P1	111.36(14)	C7'	C8'	P1'	110.79(15)
C7	C8	C9	118.28(17)	C7'	C8'	C9'	117.93(18)
C9	C8	P1	130.30(14)	C9'	C8'	P1'	131.26(16)
C10	C9	C8	113.42(16)	C10'	C9'	C8'	113.1(2)
C14	C9	C8	125.42(18)	C14'	C9'	C8'	125.7(2)
C14	C9	C10	121.15(18)	C14'	C9'	C10'	121.2(2)
C9	C10	Si1	108.87(13)	C9'	C10'	Si1'	109.51(16)
C11	C10	Si1	132.96(17)	C11'	C10'	Si1'	132.5(2)

C11	C10	C9	118.16(18)	C11'	C10'	C9'	118.0(3)
C10	C11	C12	120.6(2)	C12'	C11'	C10'	120.6(3)
C13	C12	C11	120.8(2)	C13'	C12'	C11'	120.8(2)
C12	C13	C14	120.2(2)	C12'	C13'	C14'	120.4(3)
C13	C14	C9	119.1(2)	C9'	C14'	C13'	119.1(3)
C18	C17	P1	121.30(17)	C18'	C17'	P1'	117.93(14)
C22	C17	P1	118.97(18)	C18'	C17'	C22'	118.93(18)
C22	C17	C18	119.7(2)	C22'	C17'	P1'	123.14(15)
C17	C18	C19	120.2(3)	C19'	C18'	C17'	120.3(2)
C20	C19	C18	120.2(3)	C20'	C19'	C18'	120.0(2)
C21	C20	C19	120.3(3)	C21'	C20'	C19'	120.4(2)
C20	C21	C22	120.4(3)	C20'	C21'	C22'	119.8(2)
C17	C22	C21	119.3(3)	C17'	C22'	C21'	120.6(2)

NMR data

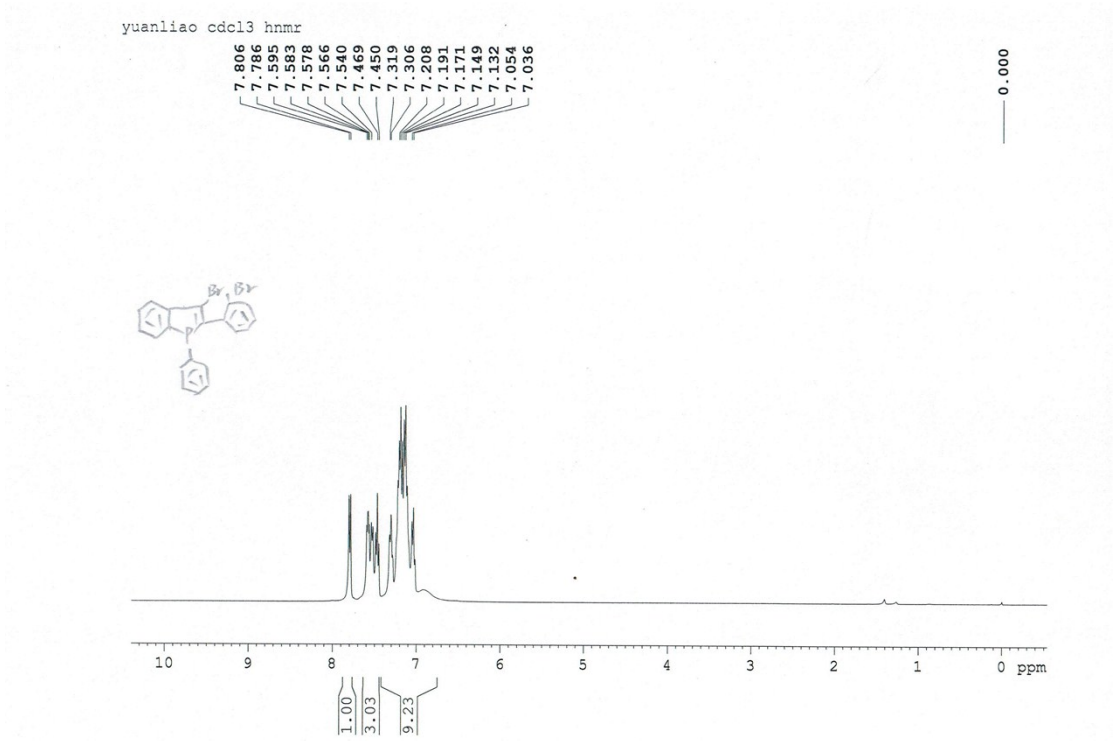

Figure S5: ^{1}H NMR (400 MHz, $CDCl_3$) of **1** at 293 K.

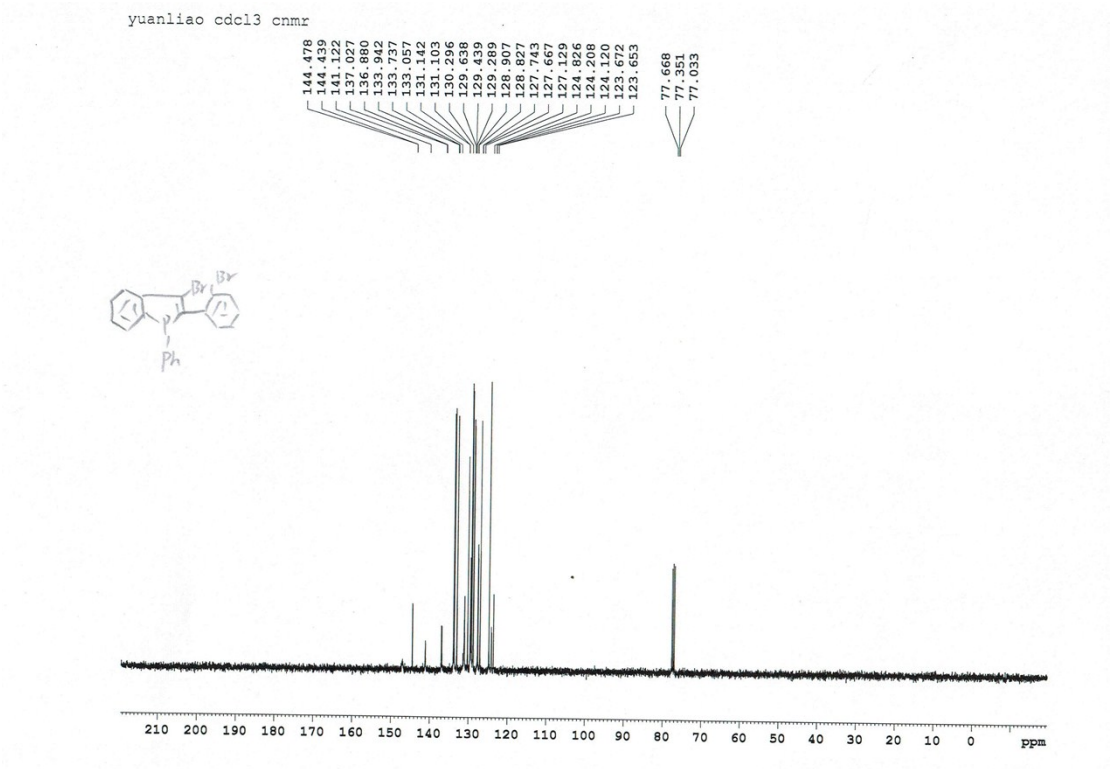

Figure S6: ^{13}C NMR (400 MHz, $CDCl_3$) of **1** at 293 K.

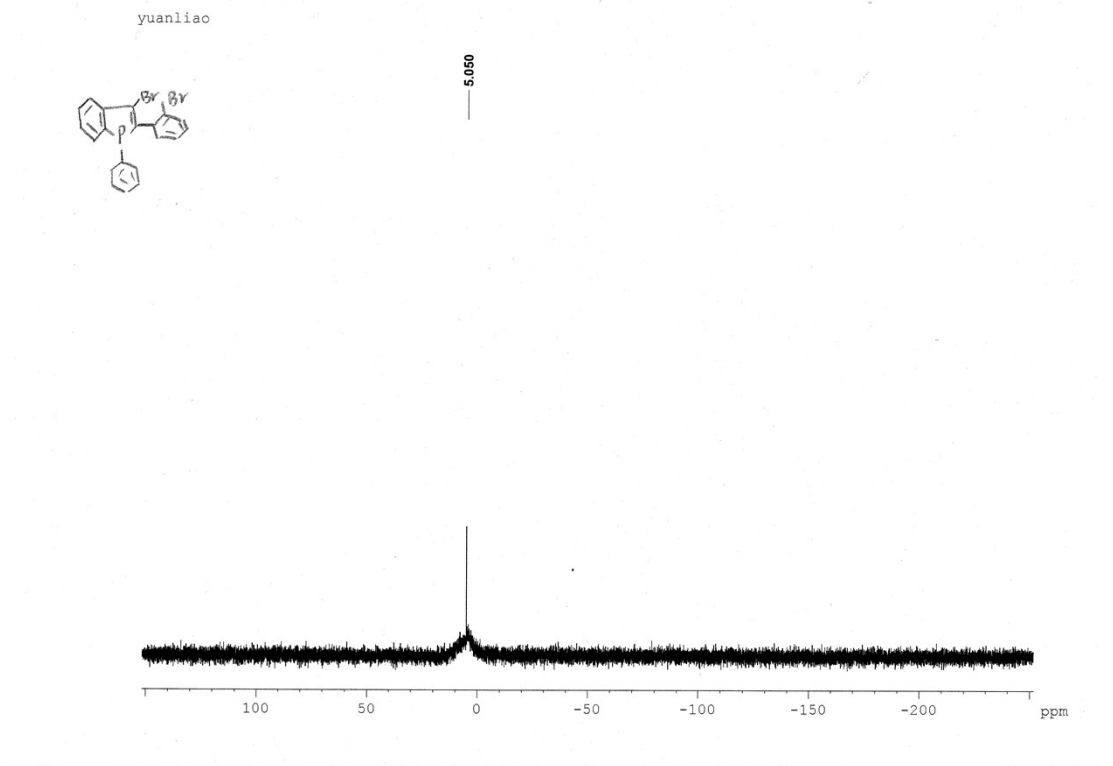

Figure S7: ^{31}P NMR (400 MHz, $CDCl_3$) of **1** at 293 K.

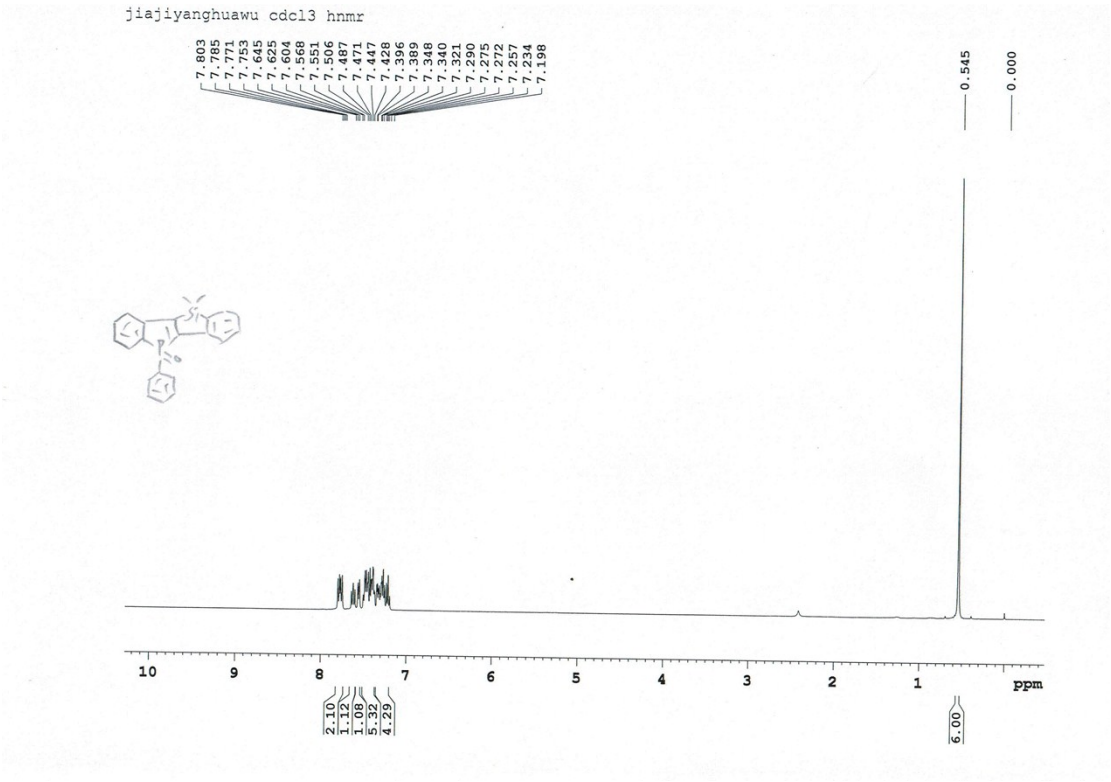

Figure S8: ^{1}H NMR (400 MHz, $CDCl_3$) of **3aO** at 293 K.

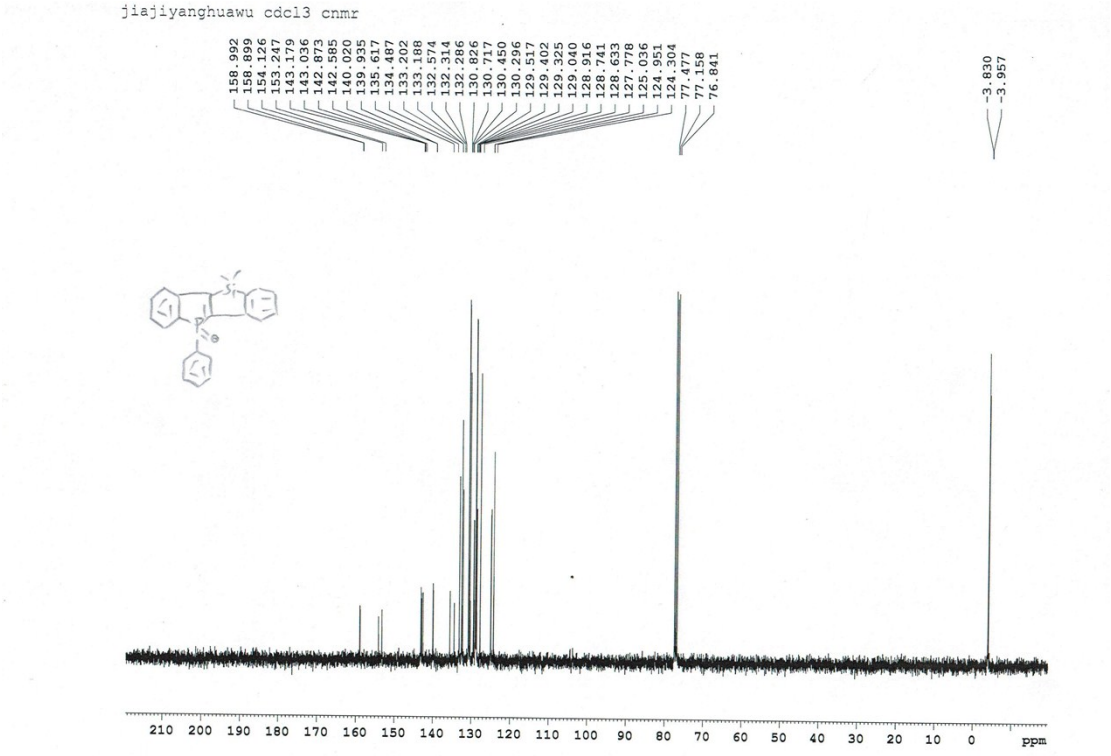

Figure S9: ^{13}C NMR (400 MHz, $CDCl_3$) of **3aO** at 293 K.

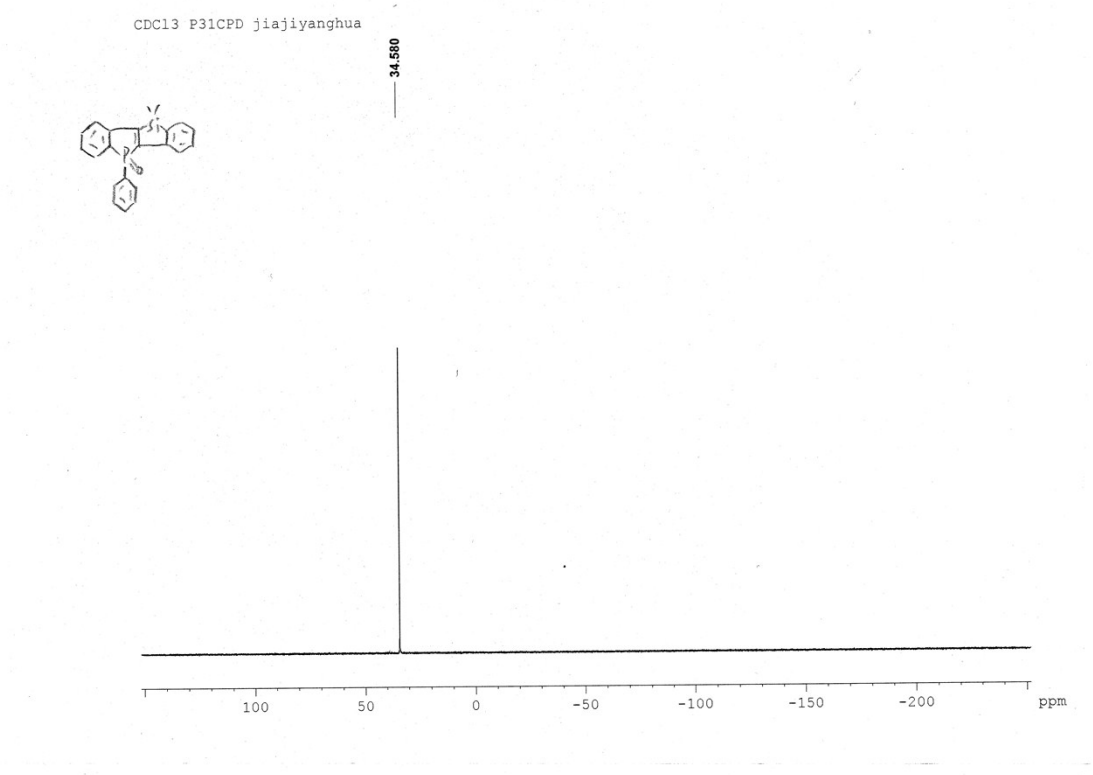

Figure S10: ^{31}P NMR (400 MHz, $CDCl_3$) of **3aO** at 293 K.

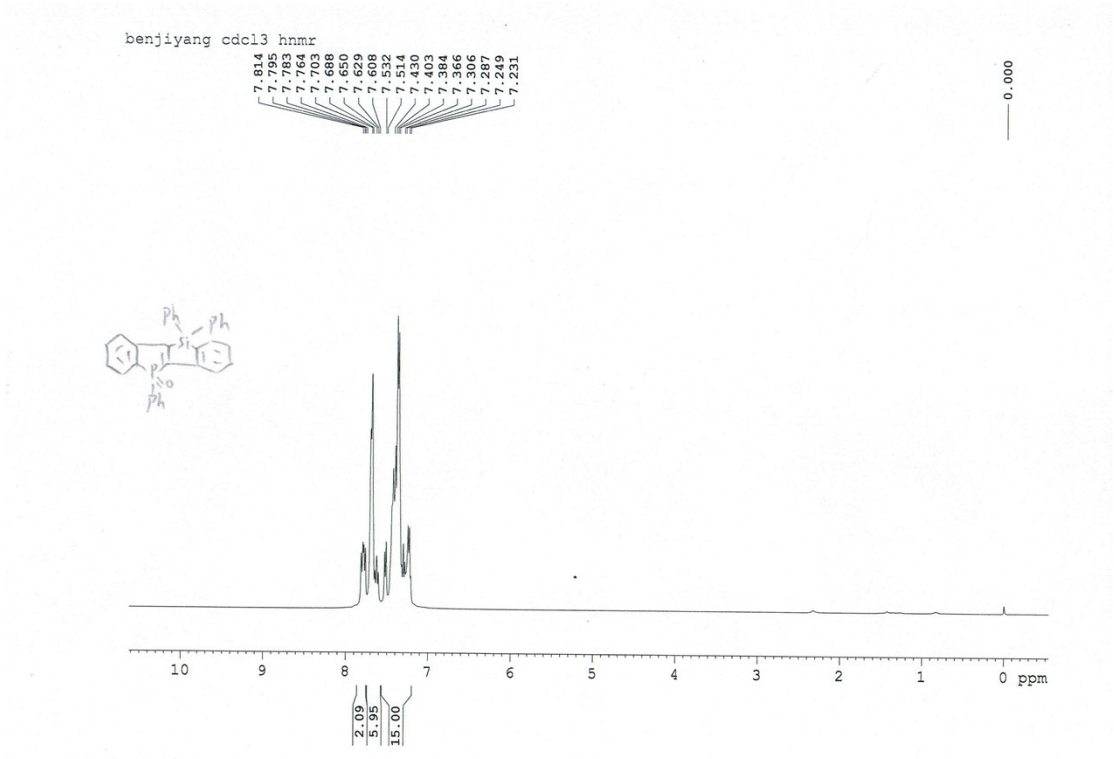

Figure S11: ^{1}H NMR (400 MHz, $CDCl_3$) of **3bO** at 293 K.

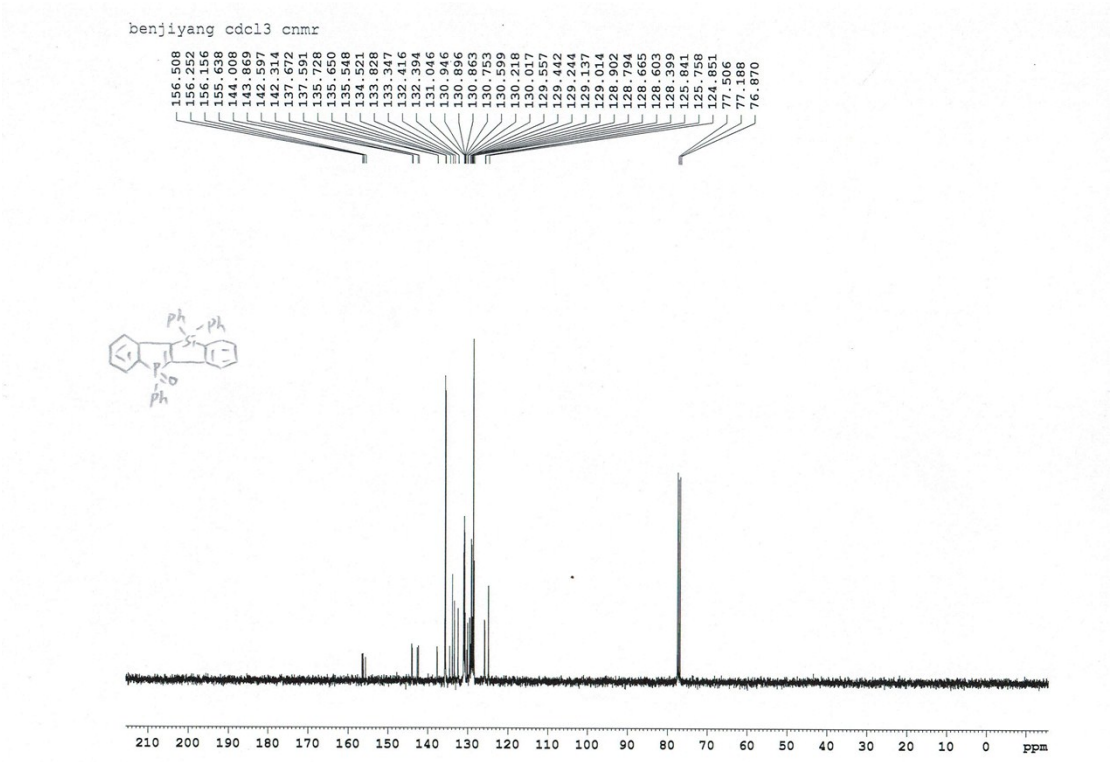

Figure S12: ^{13}C NMR (400 MHz, $CDCl_3$) of **3bO** at 293 K.

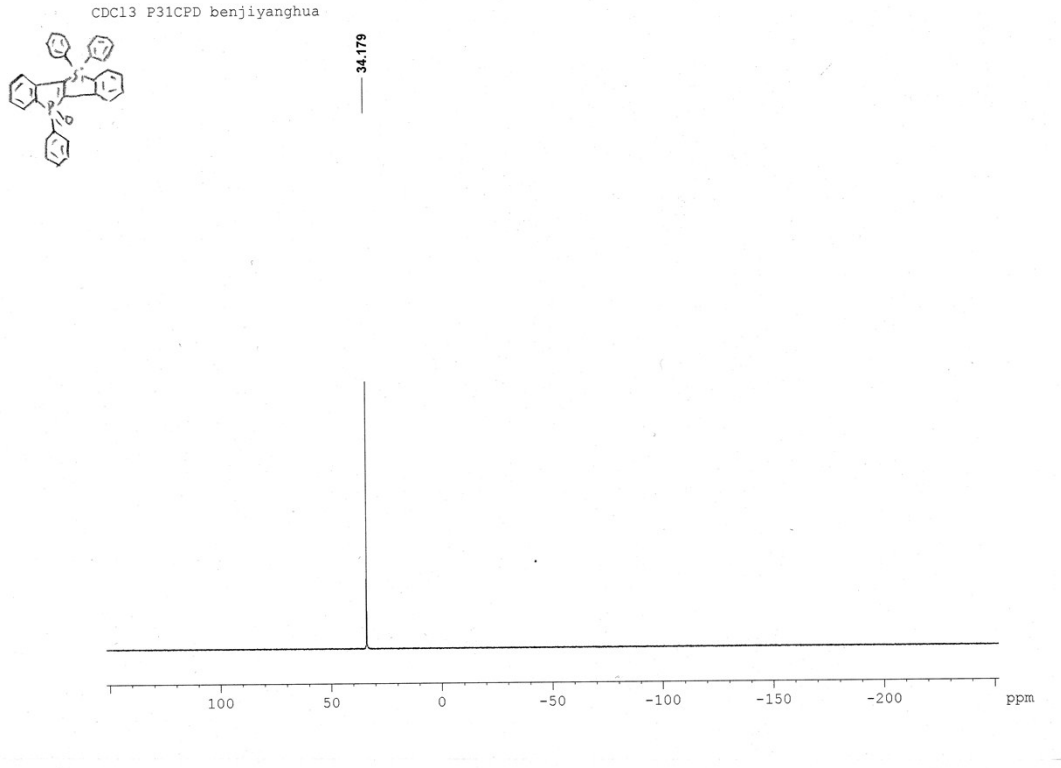

Figure S13: ^{31}P NMR (400 MHz, $CDCl_3$) of **3bO** at 293 K.

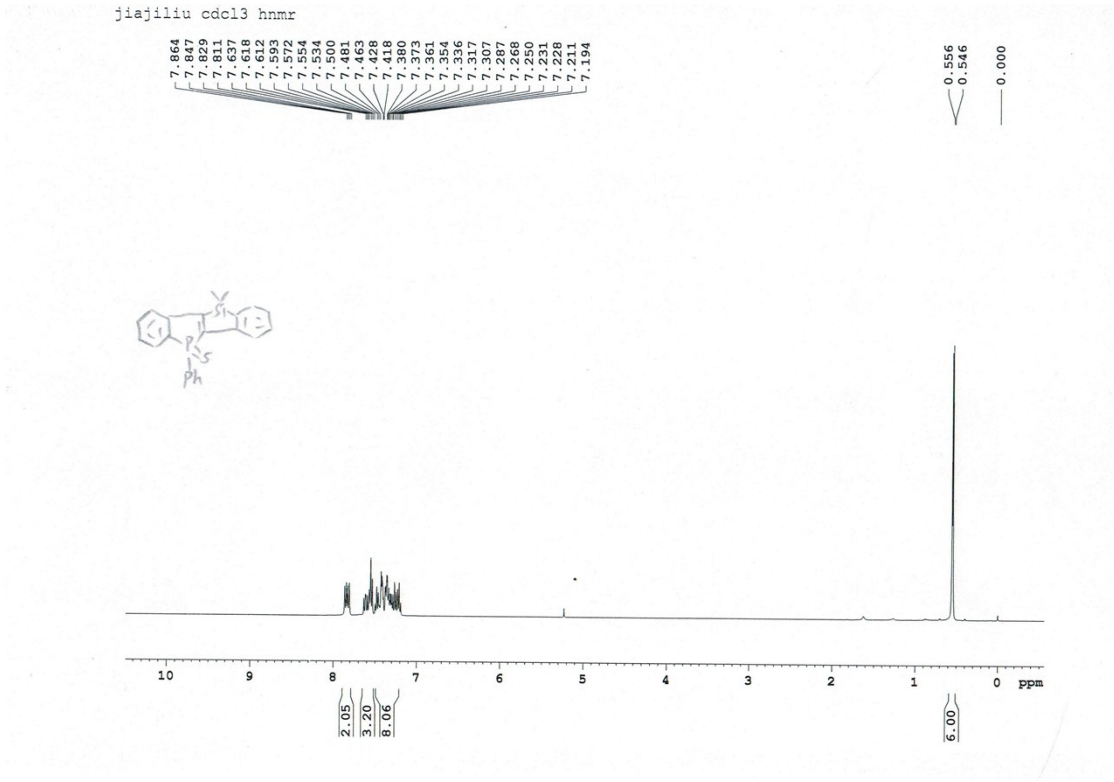

Figure S14: ^{1}H NMR (400 MHz, $CDCl_3$) of **3aS** at 293 K.

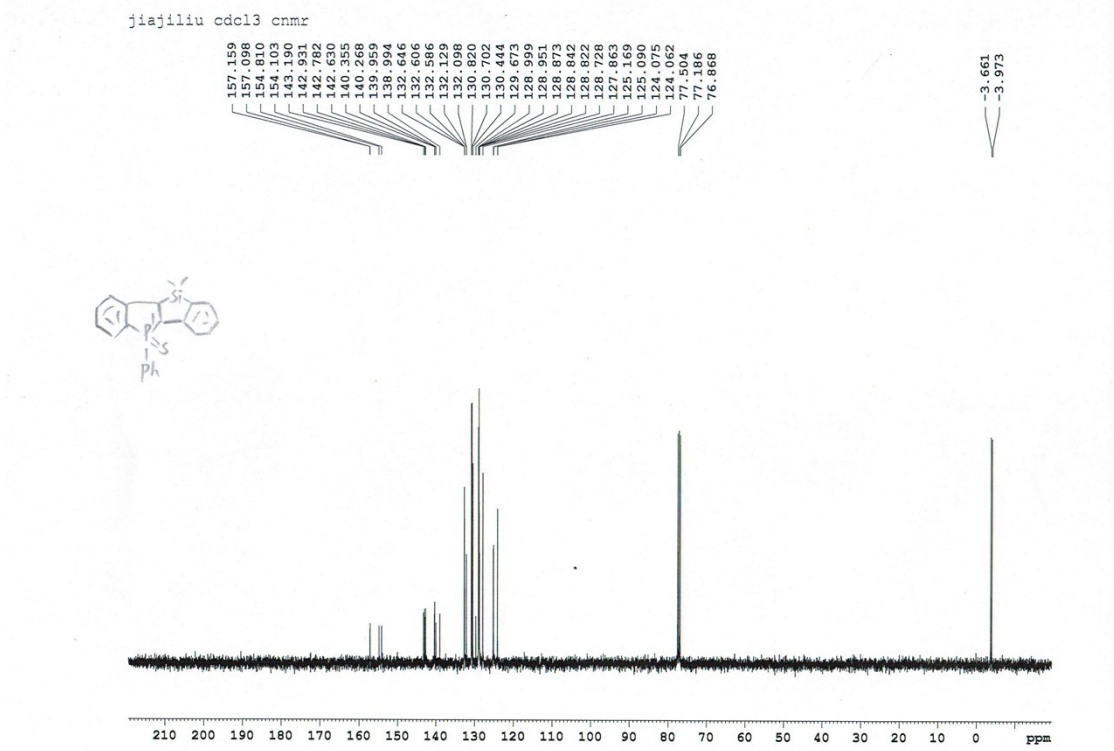

Figure S15: ^{13}C NMR (400 MHz, $CDCl_3$) of **3aS** at 293 K.

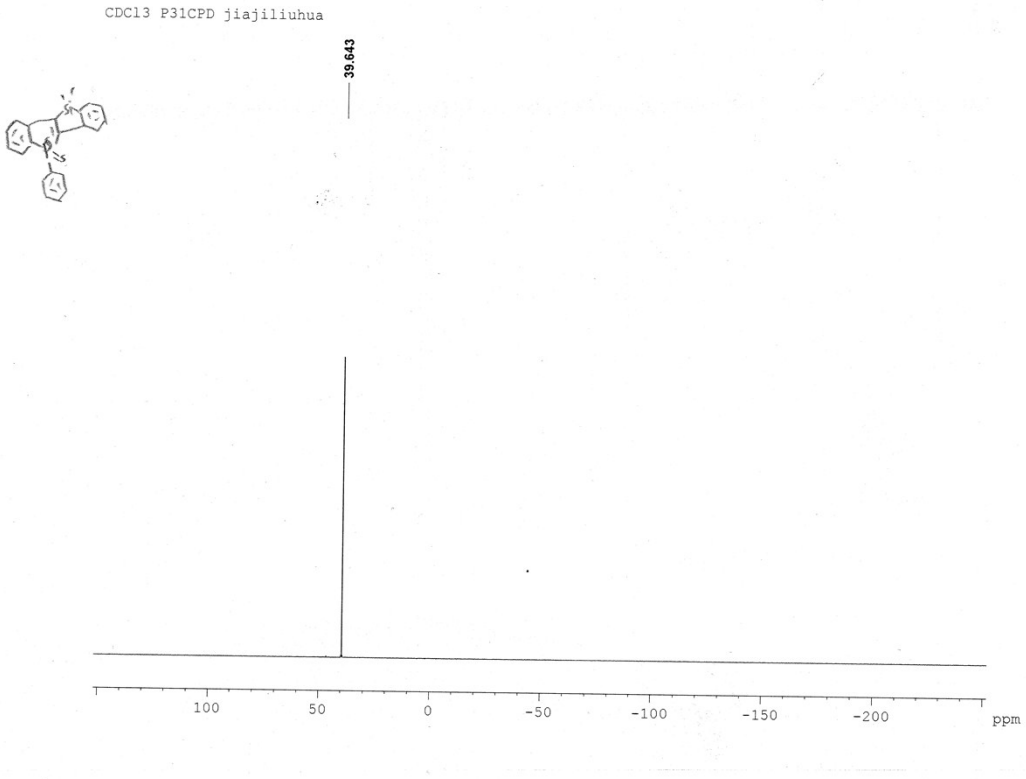

Figure S16: ^{31}P NMR (400 MHz, $CDCl_3$) of **3aS** at 293 K.

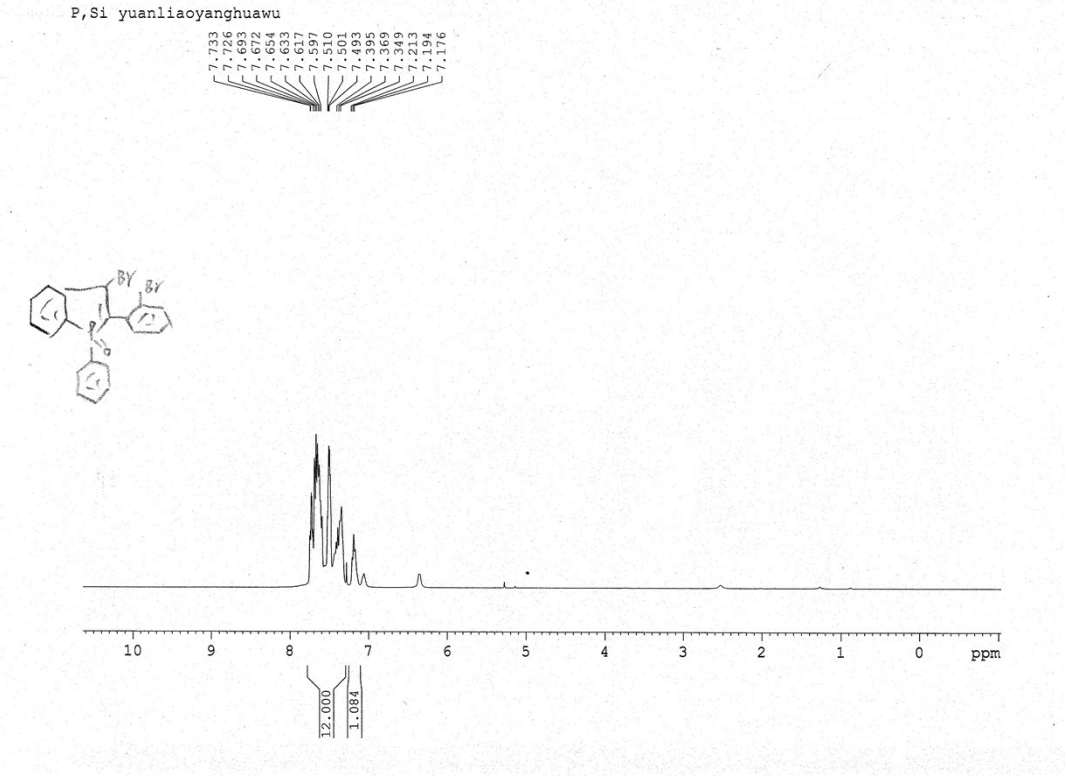

Figure S17: ^{1}H NMR (400 MHz, $CDCl_3$) of **5** at 293 K.

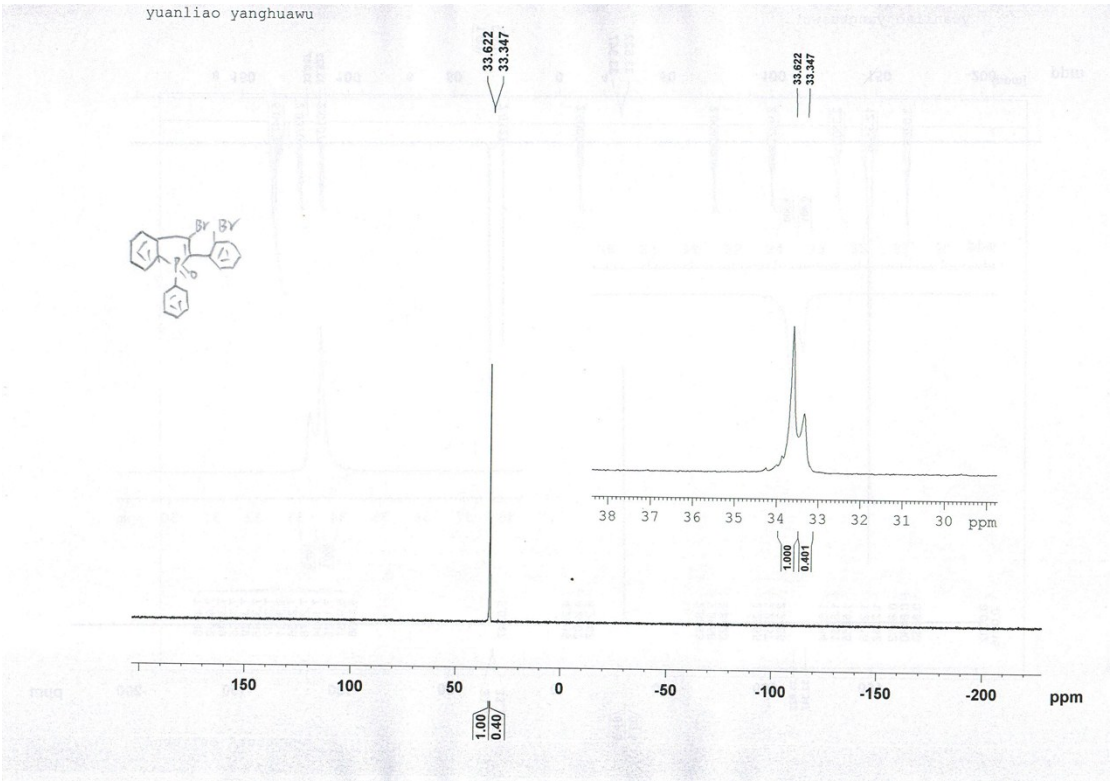

Figure S18: ^{31}P NMR (400 MHz, $CDCl_3$) of **5** at 293 K.